

# Extensive weight loss can reduce immune age by altering IgG N-glycosylation

Valentina L Greto<sup>1\*</sup>, Ana Cvetko<sup>2\*</sup>, Tamara Štambuk<sup>3\*</sup>, Niall J Dempster<sup>4</sup>, Domagoj Kifer<sup>2</sup>, Helena Deriš<sup>3</sup>, Ana Cindrić<sup>3</sup>, Frano Vučković<sup>3</sup>, Mario Falchi<sup>5</sup>, Richard S Gillies<sup>6</sup>, Jeremy W Tomlinson<sup>4</sup>, Olga Gornik<sup>2,3</sup>, Bruno Sgromo<sup>6</sup>, Tim D Spector<sup>5</sup>, Cristina Menni<sup>5\*</sup>, Alessandra Geremia<sup>1\*</sup>, Carolina V Arancibia-Cárcamo<sup>1\*</sup>, Gordan Lauc<sup>2,3\*</sup>

<sup>1</sup>Translational Gastroenterology Unit, Nuffield Department of Medicine, University of Oxford, United Kingdom

<sup>2</sup>Faculty of Pharmacy and Biochemistry, University of Zagreb, Zagreb, Croatia

<sup>3</sup>Genos Glycoscience Research Laboratory, Zagreb, Croatia

<sup>4</sup>Oxford Centre for Diabetes, Endocrinology and Metabolism, Radcliffe Department of Medicine, University of Oxford, United Kingdom

<sup>5</sup>The Department of Twin Research, King's College London, St Thomas' Hospital, London, United Kingdom

<sup>6</sup>Department of Upper GI Surgery, Oxford University Hospitals, United Kingdom

\*The authors equally contributed to this work

Corresponding author:

Gordan Lauc

[glauc@pharma.hr](mailto:glauc@pharma.hr)

Faculty of Pharmacy and Biochemistry, University of Zagreb

A. Kovačića 1, 10 000 Zagreb, Croatia

1 **ABSTRACT**

2 **Background**

3 Obesity represents a global health threat, and is associated not only with exponentially  
4 increased cardiometabolic morbidity and mortality, but with adverse clinical outcomes in  
5 patients infected with SARS-CoV-2 as well. Enzymatic attachment of complex oligosaccharides  
6 to proteins (glycosylation) is highly responsive to numerous (patho)physiological conditions  
7 and ageing, which is perhaps best exemplified on IgG. The prospect of immune age reduction,  
8 by reverting induced glycosylation changes through metabolic intervention, opens many  
9 possibilities. Herein, we have investigated whether weight loss interventions affect  
10 inflammation- and ageing-related glycosylation alterations, in a longitudinal cohort of  
11 bariatric-surgery patients. To support potential findings, BMI-related glycosylation changes  
12 were monitored in a longitudinal TwinsUK cohort.

13 **Methods**

14 IgG and plasma N-glycans were chromatographically profiled in 37 obese patients, subjected  
15 to low-calorie diet and then to bariatric surgery, across multiple timepoints. Similarly, plasma  
16 glycome was analysed in 1,680 TwinsUK participants and longitudinally monitored during a  
17 20-year follow-up.

18 **Findings**

19 Low-calorie diet induced marked increase in low branched and significant decrease in highly  
20 branched, more complex plasma N-glycans – the change opposite to the one typically  
21 observed in inflammatory conditions. Bariatric surgery resulted in extensive, gradual  
22 alterations in IgG glycome, that accompanied progressive weight loss during one year follow-  
23 up. We observed significant increase in digalactosylated and sialylated, and substantial  
24 decrease in agalactosylated and core fucosylated IgG glycans. In general, such IgG glycan  
25 profile is associated with a younger biological age and reflects enhanced anti-inflammatory  
26 IgG potential. The TwinsUK cohort replicated weight loss-associated agalactosylation decrease  
27 and digalactosylation increase, estimated through BMI decrease over a 20-year-period.

28 **Interpretation**

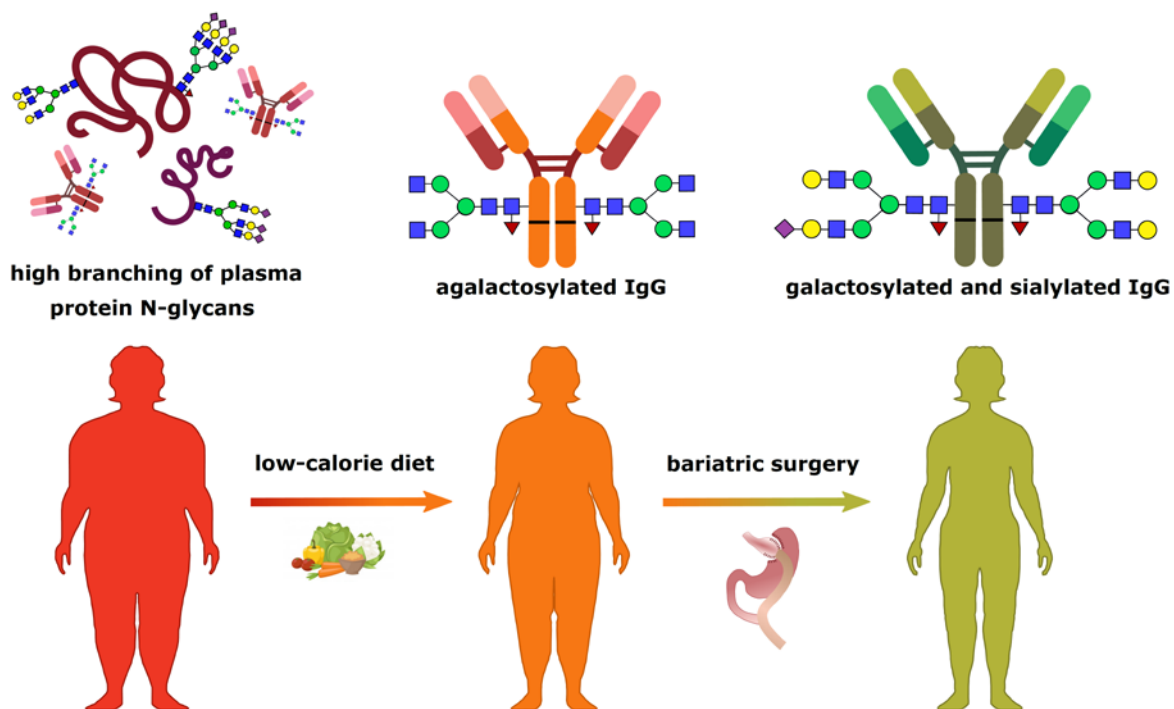
29 Altogether, these findings highlight that weight loss substantially affects both plasma and IgG  
30 N-glycosylation, resulting in improved biological and immune age.

31

32

33 **GRAPHICAL ABSTRACT**

34



35

36

37

38 **HIGHLIGHTS**

39

- 40 • Obesity is associated to circulating pro-inflammatory high branched N-glycans and  
41 IgG agalactosylation
- 42
- 43 • High branching of N-glycans from total plasma proteins decreases after 3-week low-  
44 calorie diet
- 45
- 46 • IgG galactosylation and sialylation increase after bariatric surgery-induced weight  
47 loss
- 48
- 49 • Decrease of BMI over time is associated with increased IgG galactosylation and  
50 improvement of biological age

51

52

53 **KEYWORDS**

54 N-glycosylation; bariatric surgery; weight loss; immunoglobulin G; COVID-19; biological age

## 55 INTRODUCTION

56 The global prevalence of obesity has risen dramatically, to the point that it is now considered  
57 a pandemic (1). In the current collision with the emergent coronavirus disease (COVID-19  
58 pandemic), there is a strong association of obesity and older age with COVID-19 complications  
59 and severity (2). According to the World Health Organization, over 650 million individuals are  
60 obese, accounting for the 13% of the world's adult population. Obesity confers a risk for  
61 metabolic syndrome, contributing to type 2 diabetes and cardiovascular disease (CVD)  
62 development (3). Metabolic syndrome is linked to a chronic systemic low-grade inflammation,  
63 which contributes to the aging of the immune system denoted as inflammaging (4,5). Obesity-  
64 related inflammaging results in impaired innate and adaptive immune function, and is  
65 characterized by high serum levels of IL-6, TNF- $\alpha$  and CRP (6). Moreover, this persistent  
66 inflammatory state may potentially lead to increased viral shedding and to delayed, blunted  
67 antiviral responses to SARS-CoV-2 infection (7,8).

68 Changes in protein N-glycosylation are one of the hallmarks of inflammaging (5,8). The human  
69 circulating N-glycome represents the entire set of glycans that are covalently attached to  
70 plasma proteins through a nitrogen on an asparagine residue. N-glycans are essential for life  
71 and are involved in many physiological processes (9), including signal transduction, protein  
72 trafficking and folding, receptor regulation and cell adhesion. Glycosylation has a fundamental  
73 role in the innate and adaptive immune responses, accentuated by the fact that all five classes  
74 of immunoglobulins (Ig) bear N-glycans. In this regard, IgG is probably the most investigated  
75 glycoprotein, whose effector functions are controlled by its Fc-bound glycans (10).

76 Inter-individual differences in the pace of biological ageing is an intriguing concept that tries  
77 to explain why some people stay healthy until very late chronological age, while others age  
78 faster and have shorter life expectancy. The same may apply for the risk of severe COVID-19.  
79 Progressive age-related changes of IgG glycosylation have been extensively studied (9,11,12),  
80 and the GlycanAge model has been proposed to express the difference between chronological  
81 ageing and IgG glycome ageing (13). The "age" of the IgG glycome might be estimated through  
82 the levels of agalactosylated species, which are increasing with ageing and are associated with  
83 enhanced immune activation (14). The opposite applies for digalactosylated IgG glycoforms,  
84 which are usually related to a younger age. Besides age-related changes, specific IgG  
85 glycosylation patterns have been already associated with CVD risk score and subclinical  
86 atherosclerosis in two large independent UK cohorts (15). Moreover, a prospective follow-up

87 of the EPIC-Potsdam cohort confirmed that changes in plasma N-glycome composition are  
88 predictive of future CVD events, with comparable predictive power to the American Heart  
89 Association (AHA) score in men and even better predictive power in women (16). The link  
90 between an “old”, proinflammatory IgG N-glycome and hypertension has also been  
91 profoundly studied (17–19), and similar IgG glycosylation patterns were associated with  
92 increased body mass index (BMI) and measures of central adiposity (20,21).

93 Studies on mouse models further corroborate the importance of differential IgG glycoforms  
94 in CVD pathogenesis. Namely, it has been shown that hyposialylated IgG (corresponding to an  
95 “old” IgG glycome) can induce obesity-related hypertension and insulin resistance in B-cell-  
96 deficient mice, through activation of the endothelial FcγRIIB (22,23). These findings indicate  
97 that the IgG N-glycome could represent more than a biomarker of inflammation and aging,  
98 since distinctive IgG glycoforms act as effector molecules in certain pathologies. Furthermore,  
99 supplementation with *N*-acetylmannosamine (ManNAc), a precursor of sialic acid, protects  
100 obese mice from hypertension and insulin resistance induction by reverting an “old” IgG N-  
101 glycome into a “young” one (23,24). However, studies exploring the possibilities of converting  
102 an “old” IgG glycome into a “young” one by metabolic intervention in humans are limited. Of  
103 note, only one small study indicated that high-intensity interval training can “rejuvenate” the  
104 IgG N-glycome (25).

105 Finally, severe obesity can be resolved only through bariatric surgery and subsequent weight  
106 loss (26). The resulting weight loss impacts energy balance and metabolism, contributing to  
107 the increased insulin response, improved glycaemic control and reduction of total body fat,  
108 leading to decreased CVD risk and mortality (27). In this study we aimed to determine whether  
109 weight loss affects glycan markers related to inflammation and ageing, in a longitudinally-  
110 monitored cohort of obese individuals undergoing low-calorie diet and then bariatric surgical  
111 interventions. In order to support potential findings, we also investigated the BMI-related  
112 glycosylation changes in a longitudinal TwinsUK cohort. The analysis of samples obtained from  
113 the largest longitudinal twins cohort in the UK allowed us to observe the changes of BMI in  
114 relation to the IgG N-glycosylation alterations over time.

115

## 116 **METHODS**

### 117 **Study populations**

118 *Bariatric cohort.* The cohort included 37 participants, recruited at Oxford University Hospitals  
 119 to the Gastrointestinal Illnesses study (Ref: 16/YH/0247). All patients were characterised by  
 120 metabolic status and medical history. Bariatric patients were considered eligible in accordance  
 121 to National Institute for Health and Care Excellence (NICE) and local guidelines. The choice of  
 122 bariatric operation was decided according to the Oxford Bariatric Unit regular practice.  
 123 Patients with a history of alcoholism and/or ongoing anticoagulant treatment were excluded.  
 124 Patients were also excluded in case of pregnancy, active substance abuse or uncontrolled  
 125 psychiatric condition including eating disorders. Participants were sampled at baseline and  
 126 subjected to 3-week low calorie carbohydrate-restricted diet (900 cal, maximum 100 g of  
 127 carbohydrates per day), followed by bariatric surgery. The sequential follow-up timepoints  
 128 included the day of the surgery (baseline), after  $6.54 \pm 3.4$  months (mean  $\pm$  IQR) and  $12.47 \pm$   
 129  $6.55$  months post-op. Characteristics of the bariatric cohort are shown in Table 1.

130 **Table 1 Demographic characteristics of the bariatric cohort**

<i>Characteristics</i>	<i>Bariatric cohort</i>				
Total No. of participants (N)	37				
No. of participants Sleeve Gastrectomy (SG), N (%)	25 (68%)				
No. Roux-en-Y Gastric Bypass RYGB N (%)	12 (32%)				
No. of participants each timepoint (N)	Pre-op low-calorie diet		Time of surgery	1st post-op timepoint	2 <sup>nd</sup> post-op timepoint
	8		37	30	24
BMI* each timepoint, mean $\pm$ SD, kg/m <sup>2</sup>	Before diet	End of diet	Time of surgery	1 <sup>st</sup> post-op timepoint	2 <sup>nd</sup> post-op timepoint
	$48.53 \pm 4.13$	$46.60 \pm 4.21$	$46.21 \pm 4.75$	$36.01 \pm 5.07$	$32.82 \pm 5.17$
Female, sex, N (%)	33 (89%)				
Type 2 diabetes, N (%)	6 (16%)				

131  
 132 \*BMI reference values: <18.5 (underweight), 18.5–24.9 (normal weight), 25–29.9  
 133 (overweight), >30 (obese).

134  
 135 *TwinsUK cohort.* We have analysed a total of 6,032 plasma samples from 2,146 participants of  
 136 the TwinsUK study, collected at multiple timepoints over a 20 year-period (28). These included  
 137 1,865 individuals sampled at 3 timepoints, 156 individuals sampled at 2 timepoints and 125  
 138 individuals sampled only once. Following the plasma N-glycome analysis, glycan data  
 139 underwent quality control (see *Statistical analysis* section), which decreased the dataset to  
 140 5,889 samples (measurements). Out of these 5,889 measurements, we have proceeded with

141 statistical analysis on a subset of 3,742 samples (measurements) which had information on  
142 BMI available. Description of the TwinsUK cohort is provided in Table 2.

143

144 **Table 2 Demographic characteristics of the TwinsUK cohort**

<i>Characteristics</i>	<i>TwinsUK cohort (BMI subset)</i>
No. of participants (N)	1,680
No. of glycan measurements (N)	3,742
Baseline age, mean $\pm$ SD, years	53.23 $\pm$ 10.86
Follow up time, mean $\pm$ SD, years	7.90 $\pm$ 5.66
Female sex, N (%)	1,680 (100)
Baseline BMI, mean $\pm$ SD, kg/m <sup>2</sup>	25.45 $\pm$ 4.53

145

#### 146 **Ethical statement**

147 Ethical approval for the study was obtained by the National Research Ethics Committees of  
148 the UK National Health Service (NHS) under the reference number 16/YH/0247. All individuals  
149 participating in this study gave written informed consent. The TwinsUK study was approved  
150 by NRES Committee London–Westminster, and all twins provided informed written consent.

#### 151 **N-glycome analysis**

##### 152 *Isolation of IgG from human plasma*

153 IgG was isolated from plasma samples by affinity chromatography as described previously  
154 (29). In brief, IgG was isolated in a high-throughput manner, using 96-well protein G  
155 monolithic plates (BIA Separations, Slovenia), starting from 100  $\mu$ l of plasma. Plasma was  
156 diluted 7 $\times$  with phosphate buffered saline (PBS; Merck, Germany) and applied to the protein  
157 G plate. IgG was eluted with 1 ml of 0.1 M formic acid (Merck, Germany) and immediately  
158 neutralized with 1 M ammonium bicarbonate (Acros Organics, USA).

##### 159 *N-glycan release from IgG and total plasma proteins*

160 Isolated IgG samples were dried in a vacuum centrifuge. After drying, IgG was denatured with  
161 the addition of 30  $\mu$ l of 1.33% SDS (w/v) (Invitrogen, USA) and by incubation at 65  $^{\circ}$ C for 10  
162 min. Plasma samples (10  $\mu$ l) were denatured with the addition of 20  $\mu$ l of 2% (w/v) SDS  
163 (Invitrogen, USA) and by incubation at 65  $^{\circ}$ C for 10 min. From this point on, the procedure was  
164 identical for both IgG and plasma samples. After denaturation, 10  $\mu$ l of 4% (v/v) Igepal-CA630



165 (Sigma Aldrich, USA) was added to the samples, and the mixture was shaken 15 min on a plate  
166 shaker (GFL, Germany). N-glycans were released with the addition of 1.2 U of PNGase F  
167 (Promega, USA) and overnight incubation at 37 °C.

#### 168 Fluorescent labelling and HILIC SPE clean-up of released N glycans

169 The released N-glycans were labelled with 2-aminobenzamide (2-AB). The labelling mixture  
170 consisted of 2-AB (19.2 mg/ml; Sigma Aldrich, USA) and 2-picoline borane (44.8 mg/ml; Sigma  
171 Aldrich, USA) in dimethyl sulfoxide (Sigma Aldrich, USA) and glacial acetic acid (Merck,  
172 Germany) mixture (70:30 v/v). To each sample 25 µl of labelling mixture was added, followed  
173 by 2 h incubation at 65 °C. Free label and reducing agent were removed from the samples  
174 using hydrophilic interaction liquid chromatography solid-phase extraction (HILIC-SPE). After  
175 incubation samples were brought to 96% of acetonitrile (ACN) by adding 700 µl of ACN (J.T.  
176 Baker, USA) and applied to each well of a 0.2 µm GHP filter plate (Pall Corporation, USA).  
177 Solvent was removed by application of vacuum using a vacuum manifold (Millipore  
178 Corporation, USA). All wells were prewashed with 70% ethanol (Sigma-Aldrich, St. Louis, MO,  
179 USA) and water, followed by equilibration with 96% ACN. Loaded samples were subsequently  
180 washed 5× with 96% ACN. N-glycans were eluted with water and stored at – 20 °C until usage.

#### 181 Hydrophilic interaction liquid chromatography of N glycans

182 Fluorescently labelled N-glycans were separated by hydrophilic interaction liquid  
183 chromatography (HILIC) on Acquity UPLC H-Class instrument (Waters, USA) consisting of a  
184 quaternary solvent manager, sample manager and a fluorescence detector, set with excitation  
185 and emission wavelengths of 250 and 428 nm, respectively. The instrument was under the  
186 control of Empower 3 software, build 3471 (Waters, Milford, USA). Labelled N-glycans were  
187 separated on a Waters BEH Glycan chromatography column, with 100 mM ammonium  
188 formate, pH 4.4, as solvent A and ACN as solvent B. In the case of IgG N-glycans, separation  
189 method used linear gradient of 75–62% acetonitrile at flow rate of 0.4 ml/min in a 27-min  
190 analytical run. For plasma protein N-glycans separation method used linear gradient of 70–  
191 53% acetonitrile at flow rate of 0.561 ml/min in a 25-min analytical run. The system was  
192 calibrated using an external standard of hydrolysed and 2-AB labelled glucose oligomers from  
193 which the retention times for the individual glycans were converted to glucose units (GU).  
194 Data processing was performed using an automatic processing method with a traditional  
195 integration algorithm after which each chromatogram was manually corrected to maintain  
196 the same intervals of integration for all the samples. The chromatograms were all separated



197 in the same manner into 24 peaks (GP1– GP24) for IgG N-glycans and 39 peaks (GP1–GP39)  
198 for plasma protein N-glycans and are depicted in Supplementary Figure 1 and Supplementary  
199 Figure 2, respectively. Detailed description of glycan structures corresponding to each glycan  
200 peak is presented in Supplementary Table 1. Glycan peaks were analysed based on their  
201 elution positions and measured in glucose units, then compared to the reference values in the  
202 “GlycoStore” database (available at: [https ://glyco store .org/](https://glyco store .org/)) for structure assignment. The  
203 amount of glycans in each peak was expressed as a percentage of the total integrated area.  
204 For IgG glycans, in addition to 24 directly measured glycan traits, 8 derived traits were  
205 calculated, while for plasma glycans, in addition to 39 directly measured glycan traits, 16  
206 derived traits were also calculated. These derived traits average particular glycosylation  
207 features, such as galactosylation, fucosylation, bisecting GlcNAc, and sialylation. Formulas for  
208 IgG and plasma protein N-glycan derived traits for bariatric cohort are presented in  
209 Supplementary Table 2 and Supplementary Table 3, respectively. Derived trait calculations for  
210 TwinsUK cohort are presented in Supplementary Table 4.

## 211 **Statistical analysis**

212 *Bariatric cohort.* In order to remove experimental variation from the measurements,  
213 normalization and batch correction were performed on the UPLC glycan data. To make  
214 measurements across samples comparable, normalization by total area was performed. Prior  
215 to batch correction, normalized glycan measurements were log-transformed due to right-  
216 skewness of their distributions and the multiplicative nature of batch effects. Batch correction  
217 was performed on log-transformed measurements using the ComBat method (R package *sva*  
218 (30), where the technical source of variation (which sample was analysed on which plate) was  
219 modelled as batch covariate. To correct measurements for experimental noise, estimated  
220 batch effects were subtracted from log-transformed measurements.

221 Longitudinal analysis of patient samples through their observation period was performed by  
222 implementing a linear mixed effects model, where time was modelled as fixed effect, while  
223 the individual ID was modelled as random effect. Prior to the analyses, glycan variables were  
224 all transformed to standard Normal distribution by inverse transformation of ranks to  
225 Normality (R package “GenABEL”, function *rntransform*). Using rank transformed variables  
226 makes estimated effects of different glycans comparable, as these will have the same  
227 standardized variance. False discovery rate (FDR) was controlled by the Benjamini-Hochberg

228 procedure at the specified level of 0.05. Data was analysed and visualized using R  
229 programming language (version 3.5.2)(31).

230 *TwinsUK cohort*. Normalization of peak intensities to the total chromatogram area was  
231 performed for each measured sample separately. Calculated proportions were then batch  
232 corrected using ComBat method (R package *sva*)(30). After the batch correction the first 11  
233 peaks, which predominantly originate from IgG (32), were used to calculate 6 derived glycan  
234 traits – agalactosylation (G0), monogalactosylation (G1), digalactosylation (G2), bisecting  
235 GlcNAc (B), core fucosylation (CF) and high mannose structures (HM). Mixed models were  
236 fitted to estimate the effect of BMI change on IgG N-glycome (R package *lme4*)(33). Directly  
237 measured or derived glycan trait was used as a dependent variable in the mixed model. To  
238 differentiate between BMI change and the absolute BMI value, the variable was separated to  
239  $BMI_{baseline}$  and  $BMI_{difference}$  (calculated according to the following equation:  $BMI_{difference} =$   
240  $BMI_{follow\ up\ age} - BMI_{baseline\ age}$ ), and both were used in the model as a fixed effect. Since  
241 IgG N-glycome is affected by aging, age was included both as a fixed effect and a random  
242 slope. Finally, to meet the independency criteria, family ID and individual ID (nested within  
243 family) were included in the model as a random intercept. Due to multiple model fitting (for  
244 11 directly measured and 6 derived glycan traits) false discovery rate was controlled using  
245 Benjamini-Hochberg method. All statistical analyses were performed using R programming  
246 language (version 3.6.3)(31).

247

248

## 249 RESULTS

### 250 **Pre-surgical low-calorie diet extensively changes plasma N-glycome**

251 We profiled both plasma and IgG N-glycome in a cohort of bariatric surgery-candidate patients  
252 at the beginning and at the end of their pre-operative diet. We calculated corresponding  
253 derived glycan traits, which average particular glycosylation features. By employing a linear  
254 mixed model, we observed ample changes in plasma N-glycome, as 10 out of 16 calculated  
255 derived traits displayed significant alterations after the low-calorie diet. Namely, low  
256 branched (LB), agalactosylated (G0), monogalactosylated (G1), asialylated (S0),  
257 monosialylated (S1), core fucosylated (CF) and glycans bearing a bisecting GlcNAc (B) showed  
258 a substantial increase in their abundances (Table 3). Conversely, high branched (HB),  
259 trisialylated (S3) and trigalactosylated (G3) glycan abundances decreased (Table 3).

260 Interestingly, IgG glycome was not affected by the low-calorie diet, as its derived traits did not  
 261 display any significant changes after the dieting period. Graphical representation of the  
 262 longitudinal alterations in plasma N-glycome after low calorie diet are depicted in Figure 1.

263

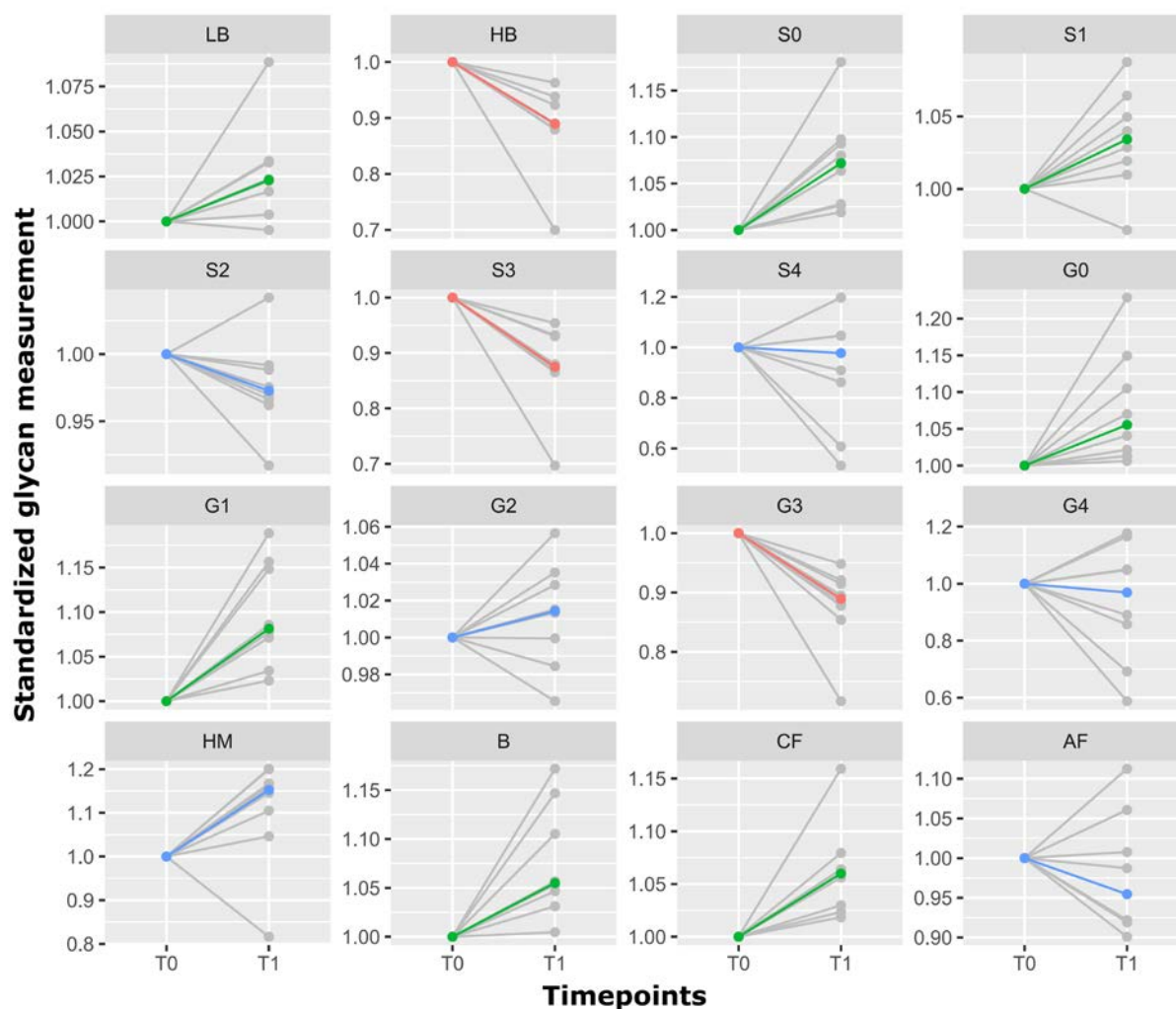
264 **Table 3 Low-calorie diet induces significant changes in plasma N-glycome.** Longitudinal  
 265 analysis was performed by implementing a linear mixed effects model, with time as a fixed  
 266 effect and the individual sample measurement as a random effect. False discovery rate was  
 267 controlled using Benjamini-Hochberg method at the specified level of 0.05.

<i>Derived glycan trait</i>	<i>Time_effect</i>	<i>Time_SE</i>	<i>Time_p-value</i>	<i>Adjusted p-value</i>
monogalactosylation (G1)	0.6020	0.0796	4.18 x10 <sup>-05</sup>	6.69 x10 <sup>-04</sup>
trisialylation (S3)	-1.1512	0.2008	3.04 x10 <sup>-04</sup>	2.43 x10 <sup>-03</sup>
agalactosylation (G0)	0.4903	0.0948	6.09 x10 <sup>-04</sup>	2.44 x10 <sup>-03</sup>
core fucosylation (CF)	0.5431	0.1011	4.73 x10 <sup>-04</sup>	2.44 x10 <sup>-03</sup>
high branching (HB)	-1.1925	0.2468	9.43 x10 <sup>-04</sup>	2.52 x10 <sup>-03</sup>
asialylation (S0)	0.6336	0.1310	9.40 x10 <sup>-04</sup>	2.52 x10 <sup>-03</sup>
trigalactosylation (G3)	-1.1925	0.2581	1.24 x10 <sup>-03</sup>	2.84 x10 <sup>-03</sup>
bisecting GlcNAc (B)	0.5457	0.1350	2.84 x10 <sup>-03</sup>	5.69 x10 <sup>-03</sup>
low branching (LB)	0.9839	0.3060	9.99 x10 <sup>-03</sup>	1.78 x10 <sup>-02</sup>
monosialylation (S1)	0.5024	0.1981	2.98 x10 <sup>-02</sup>	4.77 x10 <sup>-02</sup>
disialylation (S2)	-0.4314	0.1941	4.99 x10 <sup>-02</sup>	7.25 x10 <sup>-02</sup>
high mannose (HM)	0.7545	0.3619	6.24 x10 <sup>-02</sup>	8.33 x10 <sup>-02</sup>
antennary fucosylation (AF)	-0.1804	0.1102	1.28 x10 <sup>-01</sup>	1.58 x10 <sup>-01</sup>
digalactosylation (G2)	0.3107	0.2309	2.01 x10 <sup>-01</sup>	2.30 x10 <sup>-01</sup>
tetragalactosylation (G4)	-0.3446	0.3477	3.36 x10 <sup>-01</sup>	3.58 x10 <sup>-01</sup>
tetrasialylation (S4)	-0.3049	0.3547	4.00 x10 <sup>-01</sup>	4.00 x10 <sup>-01</sup>

268 Red – significant decrease; green – significant increase; blue – non-significant change.

269 GlcNAc – N-acetylglucosamine; SE – standard error

270



271

272 **Figure 1 Low calorie diet-related alterations in plasma N-glycome after a 3-week follow-up.**

273 Red line – significant decrease; green line – significant increase; blue line – non-significant

274 change.

275 **Bariatric surgery markedly alters IgG N-glycosylation**

276 Using the same chromatographic approach, we analysed samples from patients who

277 underwent bariatric surgery. The plasma samples were collected on the day of surgery (month

278 0), approximately 6 months post-surgery and 12 months post-surgery. Both plasma and IgG

279 N-glycans were profiled in each of these timepoints, and the obtained values were used for

280 derived glycan traits calculations. Of the examined plasma glycosylation features, only

281 agalactosylation (G0) displayed significant decrease after bariatric surgery (Table 4). On the

282 other hand, IgG N-glycome showed more extensive changes, following the bariatric

283 procedure. Namely, four out of eight tested derived traits showed marked changes: core

284 fucosylated (CF) and agalactosylated (G0) glycans decreased, while digalactosylated (G2) and

285 monosialylated (S1) glycans increased after the surgery (Table 4). The IgG glycans whose

286 abundances were increased after bariatric surgery are major components of a “young” IgG  
287 glycome, as they are typically associated with a younger age. The opposite applies to  
288 agalactosylated structures, which are usual denominators of an “old” IgG glycome profile. We  
289 also examined the correlation of patients’ clinical data with plasma and IgG glycome features  
290 using multivariate analysis, but found no statistically significant associations (data not shown).  
291 Finally, the type of bariatric surgery (either sleeve gastrectomy or Roux-en-Y gastric bypass)  
292 did not affect plasma nor IgG glycome composition. Graphical representations of the  
293 longitudinal alterations in IgG and plasma glycosylation features are depicted in Figure 2 and  
294 Supplementary Figure 3, respectively.

295

296 **Table 4 Bariatric surgery induces significant changes in plasma and IgG N-glycomes.**

297 Longitudinal analysis was performed by implementing a linear mixed effects model, with  
298 time as a fixed effect and the individual sample measurement as a random effect. False  
299 discovery rate was controlled using Benjamini-Hochberg method at the specified level of  
300 0.05.

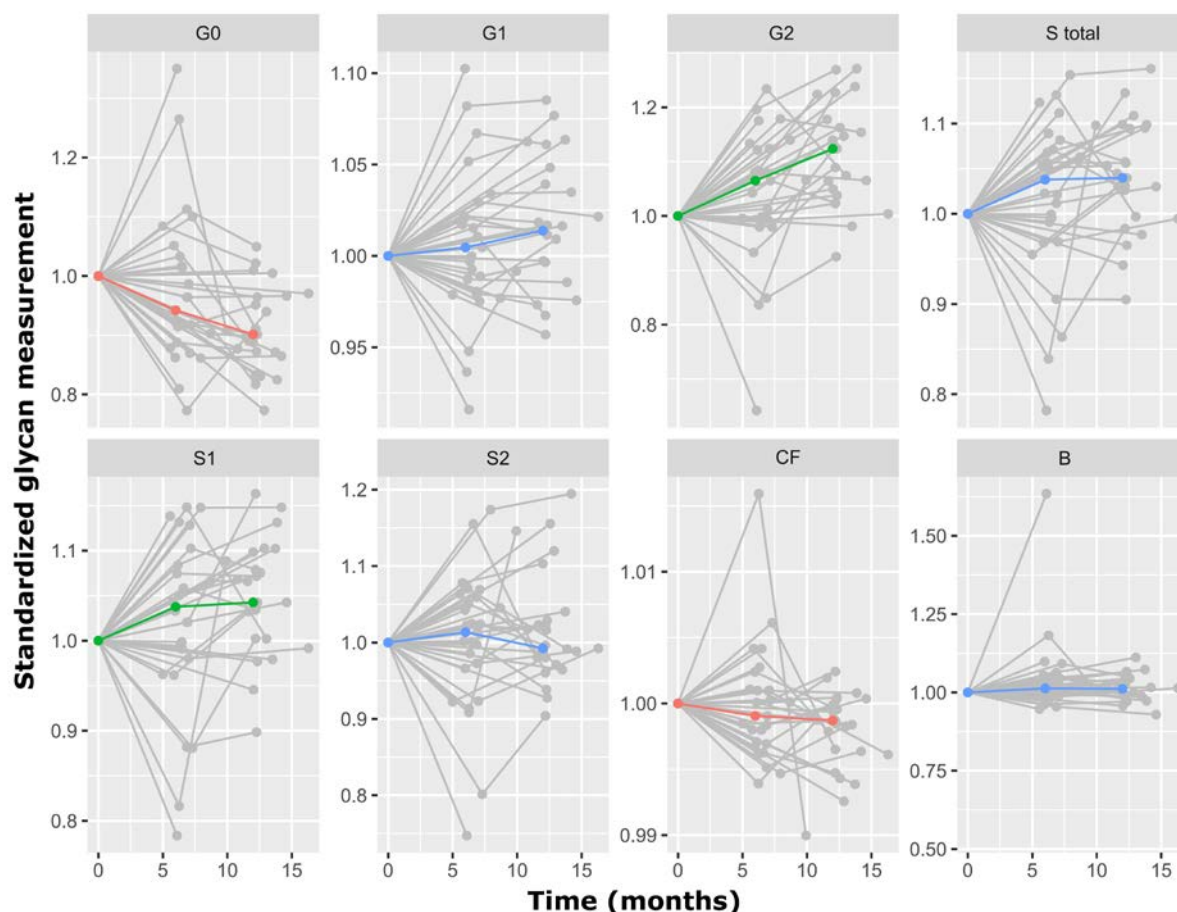
<i>N-glycome</i>	<i>Derived glycan trait</i>	<i>Time_effect</i>	<i>Time_SE</i>	<i>Time_p-value</i>	<i>Adjusted p-value</i>
plasma	agalactosylation (G0)	-0.0273	0.0071	5.26x10 <sup>-04</sup>	8.42x10 <sup>-03</sup>
IgG	agalactosylation (G0)	-0.0339	0.0078	9.23x10 <sup>-05</sup>	7.38x10 <sup>-04</sup>
IgG	digalactosylation (G2)	0.0275	0.0072	3.75x10 <sup>-04</sup>	1.50x10 <sup>-03</sup>
IgG	monosialylation (S1)	0.0193	0.0080	1.97x10 <sup>-02</sup>	3.94x10 <sup>-02</sup>
IgG	core fucosylation (CF)	-0.0155	0.0064	1.74x10 <sup>-02</sup>	3.94x10 <sup>-02</sup>

301 Red – significant decrease; green – significant increase. SE – standard error.

302

303

304



305

306 **Figure 2 Bariatric surgery-related alterations in IgG N-glycome over time (months).** Red line  
307 – significant decrease; green line – significant increase; blue line – non-significant change.

308

### 309 **Weight loss induces shift towards “young” IgG N-glycome**

310 Using the same chromatographic approach, we profiled plasma protein N-glycome from 1,680  
311 TwinsUK study participants sampled at several timepoints over a 20-year-period. This served  
312 as a replication of the findings from the bariatric cohort, whose participants exhibited the  
313 reversal from “old” to “young” IgG N-glycome due to weight loss. As these results showed  
314 prominent changes in IgG composite glycan traits only, herein we focused on IgG glycosylation  
315 changes. Due to the fact that for TwinsUK cohort plasma glycome was profiled, we calculated  
316 derived traits and performed statistical analysis only on the first 11 glycan peaks,  
317 corresponding to the glycans predominantly originating from IgG (32). Six derived traits were  
318 calculated – agalactosylation (G0), monogalactosylation (G1), digalactosylation (G2),  
319 incidence of bisecting GlcNAc (B), core fucosylation (CF) and incidence of high mannose  
320 structures (HM). We examined IgG glycome alterations associated with changes in BMI using  
321 a mixed model on a subset of 3,742 samples. Out of six examined IgG glycosylation features



322 (derived traits), three displayed significant BMI-related changes – agalactosylation (G0),  
 323 digalactosylation (G2) and incidence of high mannose structures (HM) (Table 5). Namely, the  
 324 abundance of digalactosylated (G2) glycans increased with the BMI decrease, while the  
 325 abundance of agalactosylated (G0) and high mannose glycans (HM) decreased with the weight  
 326 loss, estimated by the BMI drop. These findings are in line with the results observed in the  
 327 bariatric surgery cohort. Graphical representation of the longitudinal BMI-dependent  
 328 alterations of IgG glycosylation are depicted at Figure 3.

329

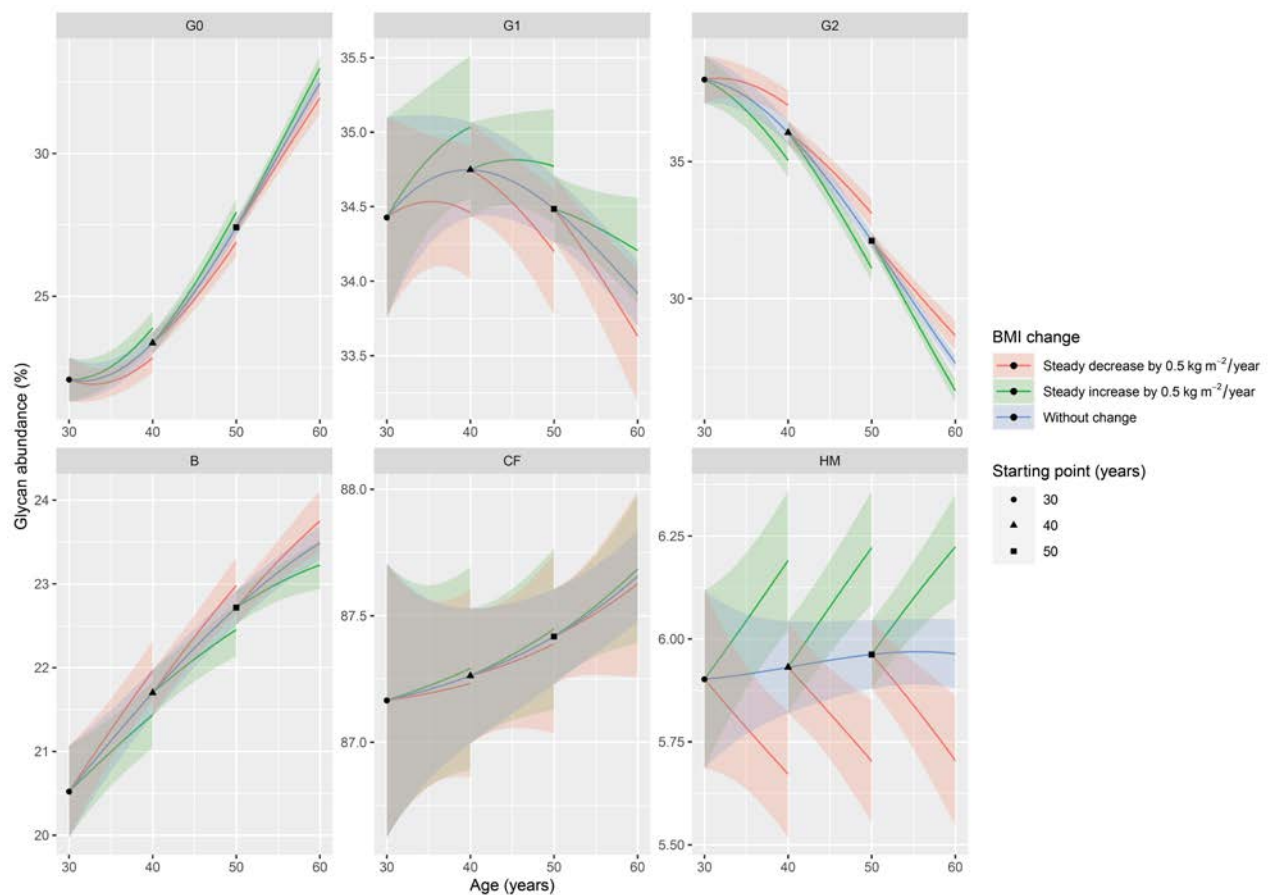
330 **Table 5 Longitudinally monitored weight loss results with significant changes of IgG N-**  
 331 **glycosylation.** Longitudinal analysis was performed by implementing a mixed model, fitted  
 332 to estimate the effect of BMI change on IgG N-glycome. False discovery rate was controlled  
 333 using Benjamini-Hochberg method at the specified level of 0.05.

<i>Derived glycan trait</i>	<i>BMI difference effect (glycan abundance (%) change per 1 kgm<sup>-2</sup> decrease in BMI)</i>	<i>BMI difference SE (glycan abundance (%) change per 1 kgm<sup>-2</sup> decrease in BMI)</i>	<i>p-value</i>	<i>Adjusted p-value</i>
digalactosylation (G2)	0.2004	0.0403	6.88x10 <sup>-07</sup>	5.85 x10 <sup>-06</sup>
high mannose (HM)	-0.0519	0.0119	1.33x10 <sup>-05</sup>	5.66 x10 <sup>-05</sup>
agalactosylation (G0)	-0.1048	0.0397	8.43x10 <sup>-03</sup>	1.79 x10 <sup>-02</sup>
bisecting GlcNAc (B)	0.0526	0.0262	4.49x10 <sup>-02</sup>	6.94x10 <sup>-02</sup>
monogalactosylation (G1)	-0.0573	0.0343	9.53x10 <sup>-02</sup>	1.25x10 <sup>-01</sup>
core fucosylation (CF)	-0.0059	0.0285	8.36x10 <sup>-01</sup>	8.89x10 <sup>-01</sup>

334 Red – significant decrease; green – significant increase; blue – non-significant change.

335 GlcNAc – N-acetylglucosamine; SE – standard error





336

337 **Figure 3 BMI-associated alterations in IgG N-glycosylation across multiple timepoints.**

338 Changes in IgG derived traits are presented with lineplots of hypothetical ageing of TwinsUK

339 participants (all women). Black dot represents a starting point of a 30-year-old woman, black

340 triangle of a 40-year-old woman and black square of a 50-year-old woman. All of these women

341 have a baseline BMI of  $25 \text{ kg m}^{-2}$ . Blue lines represent age-related IgG glycosylation changes

342 attributed to stable BMI. Green lines represent age-related IgG glycosylation changes

343 attributed to increasing BMI ( $0.5 \text{ kg m}^{-2}$  per year, through a period of 10 years). Red lines

344 represent age-related IgG glycosylation changes attributed to decreasing BMI ( $0.5 \text{ kg m}^{-2}$  per

345 year, through a period of 10 years). Highlighted areas represent 95% confidence intervals. The

346 effect of age on IgG glycosylation is represented with the curve slope, while the effect of BMI

347 change is represented with the distance of green/red line from the blue line.

348

## 349 **DISCUSSION**

350

351 In this study, we have observed extensive changes in both plasma and IgG N-glycome

352 associated with weight loss following low-calorie diet and bariatric surgery, or expressed

353 through BMI decrease. To the best of our knowledge, this is the first study to investigate

354 plasma and IgG N-glycome alterations in patients who underwent a low-calorie diet followed  
355 by bariatric surgery.

356 Prior to bariatric surgery, patients were subjected to a low-calorie diet which caused  
357 significant and extensive changes to the plasma protein N-glycome. The observed changes can  
358 be summarized as significant increase in low-branched, biantennary structures (S0, S1, G0,  
359 G1...) and, conversely, substantial decrease in high-branched, triantennary, more complex  
360 structures (S3, G3). The glycosylation alterations induced by a low-calorie diet are showing  
361 exactly the opposite direction of change than those seen in various inflammatory conditions,  
362 such as type 2 diabetes, chronic obstructive pulmonary disease and inflammatory bowel  
363 disease (16,29,34,35), suggesting a gradual attenuation of inflammation. Interestingly, no  
364 significant changes were found for the IgG N-glycome alone after the diet, probably due to  
365 the relatively short follow-up period (3 weeks), which matches IgG serum half-life. Altogether,  
366 our glycomic data suggest that the overall inflammatory body status improves after a short  
367 time of low-calorie diet, reflecting a quickly noticeable and beneficial metabolic effect.

368  
369 We have analysed both plasma and IgG N-glycome from individuals who underwent bariatric  
370 surgery, in a longitudinal manner. We observed significant changes in both plasma and IgG N-  
371 glycome. In particular, plasma N-glycome showed significant alterations only in  
372 agalactosylated (G0) glycans, whose abundance decreased during the follow-up period. Since  
373 the majority of agalactosylated species in plasma originates from IgG (32), it is no surprise that  
374 this glycosylation feature was also found to be significantly decreased in IgG glycome analysis.  
375 Elevated levels of G0 IgG glycoforms are typically associated with aging, a pro-inflammatory  
376 IgG glycan profile and various inflammatory diseases (11). On the other hand, the levels of  
377 digalactosylated (G2) glycans increased after bariatric surgery and at sequential timepoints, in  
378 accordance with a reduced inflammatory potential of the circulating IgG. Interestingly, the  
379 increased levels of IgG galactosylation are associated with a younger biological age and are  
380 considered, in a way, as a measure of an individual's well-being (14). Conversely, IgG  
381 galactosylation levels substantially decrease with ageing and during inflammation (11,13). Our  
382 results demonstrate that weight loss, resulting from bariatric surgery, can initiate the reversal  
383 from an "old" to a "young" IgG N-glycome, potentially reversing the clock for the  
384 immune/biological age. Furthermore, bariatric surgery also resulted in significant IgG glycome  
385 alteration inducing a decrease in core fucosylation. The vast majority of circulating IgG

386 molecules bears core fucose (approximately 95%), which profoundly decreases IgG binding  
387 affinity to Fc $\gamma$ RIIIA receptor and sequential antibody-dependent cellular cytotoxicity (ADCC)  
388 (36). ADCC is largely mediated by natural killer cells that can lyse target cells and fight viral  
389 infections. This would suggest that an extensive weight loss ameliorates immune responses  
390 dedicated to combat viral infections, by altering IgG glycosylation and modulating its effector  
391 functions. Lastly, bariatric surgery-related weight loss led to an increase in IgG sialylation,  
392 which is the main modulator of the IgG anti-inflammatory actions (37). In addition to its anti-  
393 inflammatory actions, the level of IgG sialylation has been implicated in the pathogenesis of  
394 obesity-induced insulin resistance and hypertension, as already mentioned (22,23). Namely,  
395 inhibitory IgG receptor Fc $\gamma$ RIIB was found to be expressed in the microvascular endothelium.  
396 Sequentially, it was shown that hyposialylated IgG acts as its operating ligand, leading to the  
397 induction of obesity-related insulin resistance and hypertension. On the other hand, the  
398 sialylated glycoform is not activating the signalling pathways responsible for the insulin  
399 resistance and hypertension development, but is rather preserving insulin sensitivity and  
400 normal vasomotor tone, even in obese mice. Interestingly, the same group made another  
401 significant discovery – promotion of IgG sialylation breaks the link between obesity and  
402 hypertension/insulin resistance (23,24). Namely, supplementation with the sialic acid  
403 precursor restored IgG sialylation, highlighting a potential approach to improve both  
404 metabolic and cardiovascular health in humans, with a single intervention. Our data suggest  
405 that a similar effect might be achieved by weight loss interventions, through restoring of IgG  
406 sialylation levels. Altogether, it is quite fascinating that such marked effects could be observed  
407 on a rather small number of participants, which further highlights their significance in a given  
408 biological setting.

409  
410 Lastly, in order to confirm the effects of weight loss on the biological/immune age, we  
411 investigated how BMI decrease affects IgG N-glycome during a 20-year-period. We observed  
412 the prominent inverse changes of agalactosylated (G0) and digalactosylated (G2) IgG glycans.  
413 Namely, agalactosylated IgG glycans significantly decreased, while digalactosylated ones  
414 substantially increased as the BMI decreased. These observations corroborated our earlier  
415 findings, confirming that the body weight reduction reverses IgG glycome from “old” to  
416 “young”, implying at the same time a likely reduction in the biological/ immune age.  
417 Nonetheless, we have to acknowledge the following limitations of TwinsUK as a replication

418 cohort: first – TwinsUK participants have not experienced such an extensive weight loss, which  
419 potentially influenced the replication of other significant glycan changes from the bariatric  
420 cohort; second – herein, the weight loss was approximated by BMI decrease, which is usually  
421 a legitimate assumption, however, it does not have to apply to all cases; and third – herein we  
422 profiled plasma glycome, while the IgG glycan traits were only approximated and the  
423 information on IgG sialylation was confounded by other plasma glycoproteins. Ideally, these  
424 issues could be circumvented in the future studies whose experimental design would allow  
425 the simultaneous, multi-centre follow-up of larger groups of patients.

426 Intense physical exercise can also shift IgG N-glycome towards a “younger” profile by  
427 increasing IgG galactosylation (25). Although another study reported that prolonged intensive  
428 exercise can have the opposite effect and promote pro-inflammatory changes of IgG N-  
429 glycome (38), its findings are not surprising since it recruited healthy, normal-weight female  
430 participants, subjected to the intense energy deprivation and exercise levels, to induce  
431 substantial fat loss in a rather short time period. The authors also highlighted that starting  
432 weight and the way in which weight loss is achieved could be crucial for the final effect on the  
433 immune system. Therefore, it seems that exercise overall has a positive impact on the immune  
434 system and biological clock, but its intensity and duration should be personalized in order to  
435 provide the optimal results.

436 To summarize, our results indicate that weight loss has impact on inflammation and biological  
437 aging by altering plasma and IgG N-glycosylation patterns. Glycosylation changes can be  
438 reliably quantified and used to estimate the “age” of the immune system. This could represent  
439 a valuable tool in the context of COVID-19 patient stratification. Since inter-individual  
440 variation in protein glycosylation is extensive, its functional implications on membrane  
441 expression of various proteins (including ACE2), functional properties of newly synthesized  
442 SARS-CoV-2 virus particles and regulation of the immune responses may also explain severe  
443 cases of COVID-19 in apparently healthy individuals. A previous research showed that  
444 impairment of ACE2 N-glycosylation affects its ability to allow the transduction of SARS Human  
445 coronavirus NL63 (HCoV-NL63) particles, by disrupting the viral endocytosis (39).

446 Future glycomic studies of patients infected with SARS- CoV-2 would help to elucidate whether  
447 ACE2 N-glycosylation differs in patients with severe COVID-19, compared to asymptomatic  
448 patients or healthy individuals.

449

450 **ACKNOWLEDGMENTS**

451 The authors thank Rachel Franklin, Michelle Haylock, James Chivenga, Roxanne Williams and  
452 Krishnageetha Manoharan for the samples collection and biobanking. The authors thank all  
453 the patients who took part in this study.

454

455 **FUNDING**

456 Glycosylation analysis was performed in Genos Glycoscience Research Laboratory and partly  
457 supported by the European Union's Horizon 2020 grants Backup (grant# 777090), European  
458 Structural and Investment Funds IRI grant (#KK.01.2.1.01.0003), Centre of Competence in  
459 Molecular Diagnostics (#KK.01.2.2.03.0006) and Croatian National Centre of Research  
460 Excellence in Personalized Healthcare grant (#KK.01.1.1.01.0010). Bariatric research was  
461 supported by the National Institute for Health Research (NIHR) Oxford Biomedical Research  
462 Centre Gastroenterology and Mucosal Immunity Theme to CVA-C and VLG, Oxford Biomedical  
463 Research Centre Diabetes and Metabolism theme for JWT, MRC programme grant to JWT (ref.  
464 MR/P011462/1), the NIHR Research Capability Funding to VLG and AG, the Wellcome Trust  
465 (101734/Z/13/Z) to AG. NJD is supported by a University of Oxford Novo Nordisk Clinical  
466 Research Fellowship. TwinsUK received funding from the Wellcome Trust European  
467 Community's Seventh Framework Programme (FP7/2007-2013 to TwinsUK); the National  
468 Institute for Health Research (NIHR) Clinical Research Facility at Guy's & St Thomas' NHS  
469 Foundation Trust and the Nottingham NIHR Biomedical Research Centre based at Guy's and  
470 St Thomas' NHS Foundation Trust and King's College London. CM is funded by the MRC AimHy  
471 (MR/M016560/1) project grant and by the Chronic Disease Research Foundation.

472

473 **AUTHOR`S CONTRIBUTION**

474 Study design: CM, AG, CVA-C, GL. Data collection: VLG, ACv, TŠ, NJD, ACi, HD, MF, CM. Data  
475 analysis: DK, FV. Data interpretation: VLG, ACv, TŠ, NJD, DK, FV, MF, JWT, OG, TS, CM, AG,  
476 CVA-C, GL. Drafting manuscript: VG, ACv, TŠ, NJD, DK, FV, GL. Revising and approving final  
477 version of manuscript: ALL. CM, AG, CVA-C and GL take responsibility for the integrity of the  
478 data analysis

479

480

481 **REFERENCES**

- 482 1. Obesity and overweight [Internet]. [cited 2020 Apr 16]. Available from:  
483 <https://www.who.int/news-room/fact-sheets/detail/obesity-and-overweight>
- 484 2. Petrilli CM, Jones SA, Yang J, Rajagopalan H, O'Donnell LF, Chernyak Y, et al. Factors  
485 associated with hospitalization and critical illness among 4,103 patients with COVID-19  
486 disease in New York City. medRxiv. 2020 Apr 11;2020.04.08.20057794.
- 487 3. Han TS, Lean ME. A clinical perspective of obesity, metabolic syndrome and  
488 cardiovascular disease. *JRSM Cardiovasc Dis*. 2016 Dec;5:2048004016633371.
- 489 4. Alpert A, Pickman Y, Leipold M, Rosenberg-Hasson Y, Ji X, Gaujoux R, et al. A clinically  
490 meaningful metric of immune age derived from high-dimensional longitudinal  
491 monitoring. *Nat Med*. 2019 Mar;25(3):487–95.
- 492 5. Franceschi C, Garagnani P, Parini P, Giuliani C, Santoro A. Inflammaging: a new  
493 immune–metabolic viewpoint for age-related diseases. *Nature Reviews Endocrinology*.  
494 2018 Oct;14(10):576–90.
- 495 6. Touch S, Clément K, André S. T Cell Populations and Functions Are Altered in Human  
496 Obesity and Type 2 Diabetes. *Curr Diab Rep*. 2017 Sep;17(9):81.
- 497 7. Dhurandhar NV, Bailey D, Thomas D. Interaction of obesity and infections. *Obes Rev*.  
498 2015 Dec;16(12):1017–29.
- 499 8. Lauc G, Sinclair D. Biomarkers of biological age as predictors of COVID-19 disease  
500 severity. *Aging* [Internet]. 2020 Apr 8 [cited 2020 Apr 14]; Available from:  
501 <http://www.aging-us.com/article/103052/text>
- 502 9. Lauc G, Pezer M, Rudan I, Campbell H. Mechanisms of disease: The human N-glycome.  
503 *Biochimica et Biophysica Acta - General Subjects*. 2016;1860(8):1574–82.
- 504 10. Gornik O, Pavić T, Lauc G. Alternative glycosylation modulates function of IgG and other  
505 proteins - implications on evolution and disease. *Biochim Biophys Acta*. 2012  
506 Sep;1820(9):1318–26.
- 507 11. Gudelj I, Lauc G, Pezer M. Immunoglobulin G glycosylation in aging and diseases.  
508 *Cellular Immunology*. 2018;
- 509 12. Dall'Olio F. Glycobiology of aging. In: *Subcellular Biochemistry*. 2018.
- 510 13. Krištić J, Vučković F, Menni C, Klarić L, Keser T, Beceheli I, et al. Glycans Are a Novel  
511 Biomarker of Chronological and Biological Ages. *The Journals of Gerontology: Series A*.  
512 2014 Jul;69(7):779–89.
- 513 14. Štambuk J, Nakić N, Vučković F, Pučić-Baković M, Razdorov G, Trbojević-Akmačić I, et al.  
514 Global variability of the human IgG glycome [Internet]. *Biochemistry*; 2019 Feb [cited  
515 2020 Jan 31]. Available from: <http://biorxiv.org/lookup/doi/10.1101/535237>



- 516 15. Menni C, Gudelj I, MacDonald-Dunlop E, Mangino M, Zierer J, Bešić E, et al.  
517 Glycosylation Profile of Immunoglobulin G Is Cross-Sectionally Associated with  
518 Cardiovascular Disease Risk Score and Subclinical Atherosclerosis in Two Independent  
519 Cohorts. *Circulation Research*. 2018;122(11):1555–64.
- 520 16. Wittenbecher C, Štambuk T, Kuxhaus O, Rudman N, Vučković F, Štambuk J, et al. Plasma  
521 N-Glycans as Emerging Biomarkers of Cardiometabolic Risk: A Prospective Investigation  
522 in the EPIC-Potsdam Cohort Study. *Diabetes Care*. 2020 Jan 7;43(3):661–8.
- 523 17. Gao Q, Dolikun M, Stambuk J, Wang H, Zhao F, Yiliham N, et al. Immunoglobulin G N-  
524 Glycans as Potential Postgenomic Biomarkers for Hypertension in the Kazakh  
525 Population. *Omics*. 2017;21(7):380–9.
- 526 18. Liu J, Dolikun M, Štambuk J, Trbojević-Akmačić I, Zhang J, Wang H, et al. The association  
527 between subclass-specific IgG Fc N-glycosylation profiles and hypertension in the  
528 Uygur, Kazak, Kirgiz, and Tajik populations. *J Hum Hypertens*. 2018 Sep;32(8–9):555–63.
- 529 19. Wang Y, Klarić L, Yu X, Thaqi K, Dong J, Novokmet M, et al. The Association Between  
530 Glycosylation of Immunoglobulin G and Hypertension: A Multiple Ethnic Cross-Sectional  
531 Study. *Medicine*. 2016 Apr;95(17):e3379.
- 532 20. Nikolac Perkovic M, Pucic Bakovic M, Kristic J, Novokmet M, Huffman JE, Vitart V, et al.  
533 The association between galactosylation of immunoglobulin G and body mass index.  
534 *Progress in Neuro-Psychopharmacology and Biological Psychiatry*. 2014 Jan;48:20–5.
- 535 21. Russell AC, Kepka A, Trbojević-Akmačić I, Ugrina I, Song M, Hui J, et al. Increased central  
536 adiposity is associated with pro-inflammatory immunoglobulin G N-glycans.  
537 *Immunobiology*. 2019;224(1):110–5.
- 538 22. Sundgren NC, Vongpatanasin W, Boggan BMD, Tanigaki K, Yuhanna IS, Chambliss KL, et  
539 al. IgG receptor FcγRIIB plays a key role in obesity-induced hypertension. *Hypertension*.  
540 2015 Feb 21;65(2):456–62.
- 541 23. Tanigaki K, Sacharidou A, Peng J, Chambliss KL, Yuhanna IS, Ghosh D, et al.  
542 Hyposialylated IgG activates endothelial IgG receptor FcγRIIB to promote obesity-  
543 induced insulin resistance. *J Clin Invest*. 2018 Jan 2;128(1):309–22.
- 544 24. Peng J, Vongpatanasin W, Sacharidou A, Kifer D, Yuhanna IS, Banerjee S, et al.  
545 Supplementation with the Sialic Acid Precursor N-acetyl-D-Mannosamine Breaks the  
546 Link Between Obesity and Hypertension. 2019.
- 547 25. Tijardović M, Marijančević D, Bok D, Kifer D, Lauc G, Gornik O, et al. Intense Physical  
548 Exercise Induces an Anti-inflammatory Change in IgG N-Glycosylation Profile. *Frontiers*  
549 *in Physiology*. 2019;10(December):1–10.
- 550 26. Nguyen NT, Kim E, Vu S, Phelan M. Ten-year Outcomes of a Prospective Randomized  
551 Trial of Laparoscopic Gastric Bypass Versus Laparoscopic Gastric Banding. *Ann Surg*.  
552 2018;268(1):106–13.



- 553 27. O'Brien P. Bariatric surgery and type 2 diabetes: a step closer to defining an optimal  
554 approach. *The Lancet Diabetes & Endocrinology*. 2019 Dec 1;7(12):889–91.
- 555 28. Verdi S, Abbasian G, Bowyer RCE, Lachance G, Yarand D, Christofidou P, et al. TwinsUK:  
556 The UK Adult Twin Registry Update. *Twin Res Hum Genet*. 2019 Dec;22(6):523–9.
- 557 29. Pavić T, Dilber D, Kifer D, Selak N, Keser T, Ljubičić Đ, et al. N-glycosylation patterns of  
558 plasma proteins and immunoglobulin G in chronic obstructive pulmonary disease. *J*  
559 *Transl Med*. 2018 Nov 21;16.
- 560 30. Leek JT, Johnson WE, Parker HS, Jaffe AE, Storey JD. The sva package for removing  
561 batch effects and other unwanted variation in high-throughput experiments.  
562 *Bioinformatics*. 2012 Mar 15;28(6):882–3.
- 563 31. R Core Team (2020). R: A language and environment for statistical computing. R  
564 Foundation for Statistical Computing, Vienna, Austria. URL [https://www.R-](https://www.R-project.org/)  
565 [project.org/](https://www.R-project.org/).
- 566 32. Clerc F, Reiding KR, Jansen BC, Kammeijer GSM, Bondt A, Wuhrer M. Human plasma  
567 protein N-glycosylation. *Glycoconj J*. 2016 Jun 1;33(3):309–43.
- 568 33. Bates D, Mächler M, Bolker B, Walker S. Fitting Linear Mixed-Effects Models Using  
569 lme4. *Journal of Statistical Software*. 2015 Oct 7;67(1):1–48.
- 570 34. Clerc F, Novokmet M, Dotz V, Reiding KR, de Haan N, Kammeijer GSM, et al. Plasma N-  
571 Glycan Signatures Are Associated With Features of Inflammatory Bowel Diseases.  
572 *Gastroenterology*. 2018;155(3):829–43.
- 573 35. Novokmet M, Lukić E, Vučković F, –Durić Ž, Keser T, Rajšl K, et al. Changes in IgG and  
574 total plasma protein glycomes in acute systemic inflammation. *Scientific Reports*. 2014  
575 Mar 11;4(1):1–10.
- 576 36. Iida S, Kuni-Kamochi R, Mori K, Misaka H, Inoue M, Okazaki A, et al. Two mechanisms of  
577 the enhanced antibody-dependent cellular cytotoxicity (ADCC) efficacy of non-  
578 fucosylated therapeutic antibodies in human blood. *BMC Cancer*. 2009 Feb 18;9:58.
- 579 37. Kaneko Y, Nimmerjahn F, Ravetch JV. Anti-Inflammatory Activity of Immunoglobulin G  
580 Resulting from Fc Sialylation. *Science*. 2006 Aug 4;313(5787):670–3.
- 581 38. Sarin HV, Gudelj I, Honkanen J, Ihalainen JK, Vuorela A, Lee JH, et al. Molecular  
582 Pathways Mediating Immunosuppression in Response to Prolonged Intensive Physical  
583 Training, Low-Energy Availability, and Intensive Weight Loss. *Front Immunol*.  
584 2019;10:907.
- 585 39. Zhao X, Guo F, Comunale MA, Mehta A, Sehgal M, Jain P, et al. Inhibition of  
586 endoplasmic reticulum-resident glucosidases impairs severe acute respiratory  
587 syndrome coronavirus and human coronavirus NL63 spike protein-mediated entry by  
588 altering the glycan processing of angiotensin I-converting enzyme 2. *Antimicrob Agents*  
589 *Chemother*. 2015 Jan;59(1):206–16.

